Journal of Magnetism and Magnetic Materials 426 (2017) 70–73

Contents lists available at ScienceDirect

Journal of Magnetism and Magnetic Materials

journal homepage: www.elsevier.com/locate/jmmm

Variation of magnetic properties with mischmetal content in the resource saving magnets of MM-Fe-B ribbons

Zhu-bai Li[a,e,*], Li-chen Wang[b,c], Xiao-peng Geng[d], Feng-xia Hu[e], Ji-rong Sun[e], Bao-gen Shen[e]

[a] *Key Laboratory of Integrated Exploitation of Bayan Obo Multi-Metal Resources, Inner Mongolia University of Science and Technology, Baotou 014010, China*

[b] *Key Laboratory of Magnetic Materials and Devices, Ningbo Institute of Material Technology and Engineering, Chinese Academy of Sciences, Ningbo 315201, China*

[c] *Laboratory of Magnetic Materials and Application Technology, Ningbo Institute of Material Technology and Engineering, Chinese Academy of Sciences, Ningbo 315201, China*

[d] *Inner Mongolia Baotou Steel Rare Earth Magnetic Materials Co.Ltd, Baotou 014030, China*

[e] *State Key Laboratory for Magnetism, Institute of Physics, Chinese Academy of Sciences, Beijing 100190, China*

ARTICLE INFO

Keywords:
Mischmetal
Permanent magnets
Phase constitution
Magnetic properties

ABSTRACT

Magnetic materials of MM-Fe-B (MM=mischmetal) ribbons were prepared using melt spinning method by varying the content of MM. The ribbons contain minor phases besides the main phase of $Re_2Fe_{14}B$. X-ray techniques show that the diffraction peak intensities of the minor phase Fe_3B vary with the content of constituent elements, indicating that the amount of minor phase could be tunable. The squareness of hysteresis loop is the best in $MM_{13}Fe_{80.5}B_{6.5}$ ribbons, which should mainly ascribe to the less amount of minor phase. Henkel plots verify the more uniform magnetization reversals in $MM_{13}Fe_{80.5}B_{6.5}$ ribbons, and the energy product achieves to the maximum of 12.74 MGOe with the coercivity of 6.50 kOe. With the increase of MM content the coercivity increases monotonically, and reaches to 9.13 kOe in $MM_{15}Fe_{77.5}B_{7.5}$ ribbons, which should be related with the nature of the defects in the main phase. These investigations show that optimizing the content of constituent elements and phase constitution could improve magnetic properties in the resource-saving magnets of MM-Fe-B ribbons.

1. Introduction

Rare earth is one of the important strategic non-renewable resources, which is widely used and pushes greatly the development of technology in new materials, energy conservation, aerospace, electronic information, environmental protection and other fields, but the reserves are limited in the mineral [1]. The rare earth mineral is multi-element paragenetic ore. La and Ce are much abundant whereas Pr and Nd are less abundant [2–4]. The mass production and wide application of $(PrNd)_2Fe_{14}B$ lead to the unbalanced utilization of rare earth elements, resulting in the over-consumption of less abundant PrNd and the overstock of the most abundant LaCe, which therefore aggravates the crisis of rare earth resource scarcity [5–8]. It is necessary to utilize rare earth elements more efficiently to reduce mine exploration for protecting natural resources as well as to decrease the production cost [9–12]. The substitution of high abundant rare earth La and Ce for Nd was investigated in the $Re_2Fe_{14}B$ magnets [13–18]. However, the mass-substitute leads to the deterioration of magnetic properties [19–21], which results not only from the intrinsic magnetic properties, i.e., the low magnetocrystalline anisotropy of $La_2Fe_{14}B$ and $Ce_2Fe_{14}B$ [22], but from the different phase diagram of Ce(La)-Fe-B from that of Nd-Fe-B [23–26]. It is that employing the addition of Nd or Ho the phase constitution could be optimized and magnetic properties are improved in $(ReCe)_2Fe_{14}B$ magnets [27,28]. Purifying the simple substance of La, Ce, Pr, Nd is high costly compared to purifying the mischmetal metal, i.e., the mixture of rare earth elements. Provided that mischmetal is used in the permanent magnets for substitution for PrNd, the rare earth could be utilized more efficiently and the cost of raw material is reduced largely [29,30]. In this letter, we prepared MM-Fe-B magnets using mischmetal (MM) by melt spinning method. The magnetic properties could be improved by optimizing the content of mischmetal without the addition of simple substance Pr and Nd, which is expected to serve as a reference for preparing the resource-saving permanent magnets with moderate performance plug-

---

[*] Corresponding author at: Key Laboratory of Integrated Exploitation of Bayan Obo Multi-Metal Resources, Inner Mongolia University of Science and Technology, Baotou 014010, China.

E-mail address: lzbgj@163.com (Z.-b. Li).

http://dx.doi.org/10.1016/j.jmmm.2016.11.067
Received 11 September 2016; Received in revised form 22 October 2016; Accepted 4 November 2016

ging the gap between those of ferrite and $(NdPr)_2Fe_{14}B$ [31].

2. Experimental procedure

The commercial La-Ce-Pr-Nd mischmetal, Fe and Fe-B were used to prepare MM-Fe-B alloys by arc-melting technique under an argon atmosphere. The atomic percent of MM is varied in the range between 10% and 15%. The purity of mischmetal is more than 99 wt%, and the natural atomic ratio is similar to that in minerals (La/Re~28.27 wt%, Ce/Re~50.46 wt%, Pr/Re~5.55 wt%, and Nd/Re~15.66 wt%). In order to make the ingots homogenous in chemical composition, they were turned over and melted at least three times. The precursor ingot was crushed into small pieces and inserted into a quartz tube. In the quartz tube there is a bottom orifice whose diameter is in the range of 0.8–1.0 mm. The ribbons were obtained by induction melting the ingot in the quartz tube and then ejected the melt onto the surface of a rotating copper wheel through the orifice by pressurized argon. For optimizing magnetic properties the wheel surface was polished using the 1000-grit paper. The phase constitution and grain size were examined by x-ray diffraction (XRD) using Cu Kα radiation. Magnetic measurements were performed with Lakeshore vibrating sample magnetometer (VSM).

3. Results and discussion

Fig. 1 shows the XRD patterns for $MM_{11}Fe_{83.5}B_{5.5}$, $MM_{12}Fe_{82}B_6$, $MM_{13}Fe_{80.5}B_{6.5}$ and $MM_{15}Fe_{77.5}B_{7.5}$ melt-spun ribbons. Using Jade software the average grain sizes are estimated to be in the range of 20–30 nm. According to the intensities of diffraction peak all the samples contain the main phase of $Re_2Fe_{14}B$, but the diffraction peaks are not very smooth and there are some weak peaks, indicating a little amount of amorphous phase and minor phases coexisting in these ribbons. In $MM_{11}Fe_{83.5}B_{5.5}$ and $MM_{12}Fe_{82}B_6$ the diffraction peaks of Fe_3B phase are much strong. For a comparison, the XRD patterns of $Nd_{12}Fe_{82}B_6$ ribbons are also shown in Fig. 1. Although $Nd_{12}Fe_{82}B_6$ ribbons also contain the minor phases of Fe_3B, $ReFe_2$, and $ReFe_7$, the diffraction peaks of $Re_2Fe_{14}B$ phase are stronger. It is noted that for optimizing the squareness of hysteresis loop the wheel velocity was 27 m/sec in melt-spinning for MM-Fe-B, larger than 23 m/sec for $Nd_{12}Fe_{82}B_6$ ribbons. However, the diffraction peaks of minor phase are stronger, implying the difficulty in the suppression for minor phase formation even by high quench rate in MM-Fe-B alloys. As those of Ce-Fe-B ribbons [26,32,33], the XRD pattern of $MM_{12}Fe_{82}B_6$ ribbons is also different from that of the conventional magnets of $Nd_2Fe_{14}B$. It can be seen that the intensities of (311), (321) and (112) peaks for Fe_3B phase become weaker with the increase of MM content. In $MM_{15}Fe_{77.5}B_{7.5}$ the peak intensities of Fe_3B phase become stronger, which may be attributed to the larger atomic percent of B. It should also be noted that the diffraction peak intensities of minor phases $ReFe_2$ and $ReFe_7$ also become a little stronger, implying an increase of their amount in $MM_{15}Fe_{77.5}B_{7.5}$ ribbons. Bearing these facts in mind, though the phase constitution of MM-Fe-B is distinct from that of Nd-Fe-B [6], the amount of minor phase could be tunable by varying the content of the constituent elements.

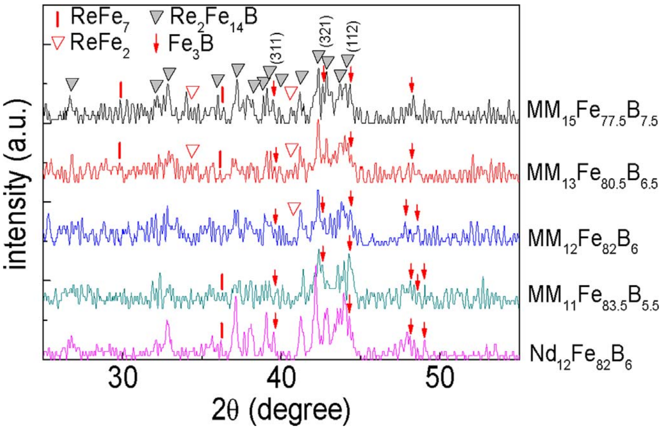

Fig. 1. XRD patterns for MM-Fe-B ribbons and $Nd_{12}Fe_{82}B_6$ ribbons.

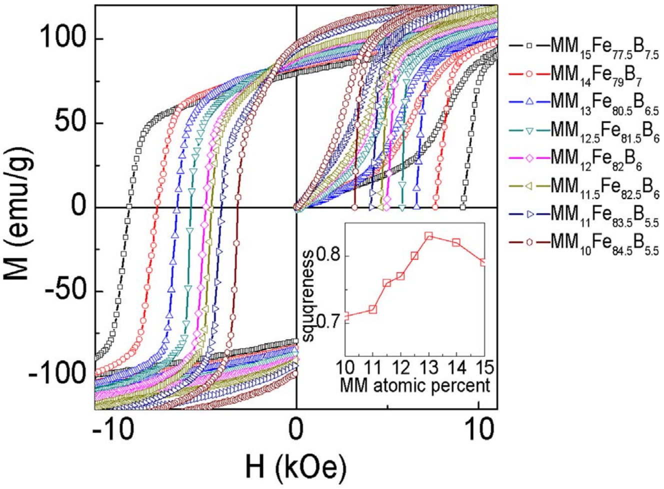

Fig. 2. The hysteresis loops for MM-Fe-B ribbons at room temperature, and the inset shows the dependence of squareness on the MM atomic percent.

The phase constitution and the microstructure severely impact on the magnetic properties. Fig. 2 shows the hysteresis loops for these optimally melt-spun MM-Fe-B ribbons. In $MM_{10}Fe_{84.5}B_{5.5}$ ribbons the coercivity is the lowest. With the increase of MM atomic percent the coercivity increases, but the remanence decreases monotonically. The decrease of remanence should ascribe to the decrease in the amount of Fe_3B phase, since Fe_3B is soft phase and possesses high saturation magnetization. In $MM_{15}Fe_{77.5}B_{7.5}$ though the amount of Fe_3B phase increases a little, the amount of minor phases $ReFe_2$ and $ReFe_7$ also increases, So the amount of main phase $Re_2Fe_{14}B$ should decrease in $MM_{15}Fe_{77.5}B_{7.5}$ ribbons, which gives rise to the decrease of remanence. The uniformity of magnetization reversal is necessary for improving the magnetic properties in permanent magnets. The squareness of hysteresis loop in second quadrant, which determined by the ratio of the integral $\int_0^{-H_c} M/M_s dH$ to M_r/M_s*H_c (the product of remanence and coercivity), can reflect the uniformity of magnetization reversal [34]. As shown in the inset of Fig. 2, with the increase of MM atomic percent the squareness is improved firstly, peaks for 13%, and then declines. The coercivity, remanence, and energy product are listed in Table 1. The largest energy product 12.74 MGOe is obtained in $MM_{13}Fe_{80.5}B_{6.5}$ ribbons, much higher than those previously reported [29,35], which suggests that the magnets with low cost and moderate performance could be prepared by mischmetal via optimizing the content of constituent elements. The well magnetic properties in $MM_{13}Fe_{80.5}B_{6.5}$ ribbons should be mainly attributed to the well squareness of hysteresis loop.

The minor phases of Fe_3B, $ReFe_2$, and $ReFe_7$ and amorphous phase

Table 1
Magnetic properties for MM-Fe-B ribbons at room temperature.

Composition	H_c (kOe)	M_r (emu/g)	Squareness	$(BH)_{max}$ (MGOe)
$MM_{10}Fe_{84.5}B_{5.5}$	3.19	96.58	0.71	8.63
$MM_{11}Fe_{83.5}B_{5.5}$	4.09	93.59	0.72	9.12
$MM_{11.5}Fe_{82.5}B_6$	4.62	90.39	0.76	10.67
$MM_{12}Fe_{82}B_6$	4.94	88.94	0.77	10.85
$MM_{12.5}Fe8_{1.5}B_6$	5.75	87.23	0.80	11.92
$MM_{13}Fe_{80.5}B_{6.5}$	6.50	84.82	0.83	12.74
$MM_{14}Fe_{79}B_7$	7.60	83.47	0.82	12.46
$MM_{15}Fe_{77.5}B_{7.5}$	9.13	79.67	0.79	11.25

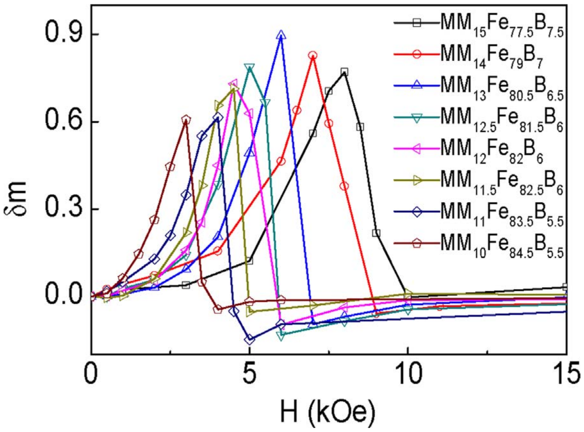

Fig. 3. δm curves (Henkel plots) for all samples at room temperature.

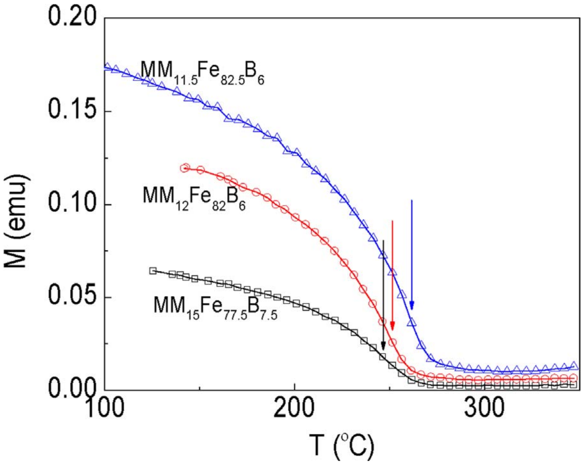

Fig. 4. Magnetization variations with temperature under the field of 1 kOe for all samples of MM-Fe-B ribbons.

are soft or paramagnetic, which probably affects the magnetic properties, since the intergranular soft phase would lead to more non-uniform magnetization reversals, resulting in the decline of the squareness degree of hysteresis loop [34]. Henkel plots, defined as $\delta m = [2M_r(H) + M_d(H)]/M_r - 1$, are also used to evaluate the intergranular exchange coupling effect and the uniformity of magnetization reversal [36]. Here $M_r(H)$ and $M_d(H)$ are the initial remanence and demagnetization remanence, respectively, and M_r is the saturation remanence. Positive value of δm suggests the existing of intergranular exchange coupling, and the large amount of soft phase would decrease the value of δm in the well exchange-coupled magnets with nanostructure. As shown in Fig. 3, the variation of δm maximum value with the MM atomic percent is consistent with that of squareness. δm value peaks a maximum of 0.89 in $MM_{13}Fe_{80.5}B_{6.5}$ ribbons, which verifies the least amount of minor phase in $MM_{13}Fe_{80.5}B_{6.5}$ among these MM-Fe-B ribbons. In Pr-Fe-B ribbons, δm value peaks a maximum of 0.91 for Pr atomic percent 12.6% in $Pr_{12.6}Fe_{81.4}B_6$ ribbons [36], and for $Nd_{12}Fe_{82}B_6$ ribbons the maximum of δm value reaches to 1.14 [27]. The difference in the variation of δm value with Re atomic percent should be partially attributed to the difference of phase constitution among MM-Fe-B, Nd-Fe-B and Pr-Fe-B. In Ce-Fe-B ribbons it is for Ce atomic percent 13.5% that δm value reaches a maximum of 0.56 [26]. It can be seen that the δm value of $MM_{13}Fe_{80.5}B_{6.5}$ is a little lower than those of Pr-Fe-B and Nd-Fe-B, but much larger than that of Ce-Fe-B ribbons. So the uniformity of magnetization reversal and squareness of hysteresis loop keep well, leading to the improvement of magnetic properties in $MM_{13}Fe_{80.5}B_{6.5}$ ribbons.

In order to further check the effect of MM content on the magnetic properties, Curie temperature was measured for $MM_{11.5}Fe_{82.5}B_6$, $MM_{12}Fe_{82}B_6$ and $MM_{15}Fe_{77.5}B_{7.5}$ ribbons, respectively. Firstly, magnetized the sample to saturation, and then increased temperature and recorded the magnetization under a magnetic field of 1 kOe (shown in Fig. 4). Curie temperature is shown by the arrow, which is determined by the abrupt change of magnetization for the increase of temperature. For $MM_{11.5}Fe_{82.5}B_6$, the magnetization doesn't decrease to zero, which should ascribe to the larger amount of Fe_3B phase that bears high Curie temperature. Even containing the same main phase, the Curie temperatures are a little different among these samples. The slight difference in Curie temperature may lie in the defects in $Re_2Fe_{14}B$ phase. The high MM content and low Fe content possibly leads to increase the vacancies in the Fe sublattices in the main phase of $Re_2Fe_{14}B$, resulting in a little decrease of the Curie temperature [26], since the decrease of Fe atomic nearest coordination number would decrease the phase transition temperature from ferromagnetic to paramagnetic state [37]. Likewise, the low MM content may lead to the increase of Re sites vacancy in $Re_2Fe_{14}B$ lattice, especially at grain outer-layer, resulting in the decrease of magnetocrystalline anisotropy. Coercivity is also dependent on the magnetocrystalline anisotropy and sensitive to the defect nature at grain outer-layer [36,38]. So the coercivity varies with the content of mischmetal in these MM-Fe-B ribbons.

4. Conclusions

In summary, the resource-saving magnets of MM-Fe-B ribbons were prepared by melt spinning method, which contain the minor phases of Fe_3B, $ReFe_2$ and $ReFe_7$ besides the main phase of $Re_2Fe_{14}B$. The amount of minor phase, which affects the squareness of hysteresis loop and the magnetic properties, is dependent on the content of constituent elements. The coercivity increases monotonically with the increase of MM content, and reaches to 9.13 kOe in $MM_{15}Fe_{77.5}B_{7.5}$ ribbons. But the amount of minor phases $ReFe_2$ and $ReFe_7$ increases, resulting in the decline of squareness degree of hysteresis loop. By optimizing the mischmetal content and phase constitution for improving the squareness of hysteresis loop, the energy product of 12.74 MGOe is obtained in $MM_{13}Fe_{80.5}B_{6.5}$ ribbons with the coercivity of 6.50 kOe. It is expected that these investigations could serve as a reference for preparing the resource-saving permanent magnets with moderate performance.

Acknowledgements

The present work was supported by the National Basic Research Program of China (Grant No. 2014CB643702) and the National Natural Science Foundation of China (Grant No. 51461033, and 51590880).

References

[1] S. Massari, M. Ruberti, Resour. Policy 38 (2013) 36.
[2] J. Jin, T. Ma, Y. Zhang, G. Bai, M. Yan, Sci. Rep. 6 (2016) 32200.
[3] A.K. Pathak, M. Khan, K.A. Gschneidner Jr., R.W. McCallum, L. Zhou, K. Sun, K.W. Dennis, C. Zhou, F.E. Pinkerton, M.J. Kramer, V.K. Pecharsky, Adv. Mater. 27 (2015) 2263.
[4] M.G. Zhu, W. Li, J.D. Wang, L.Y. Zheng, Y.F. Li, K. Zhang, H.B. Feng, T. Liu, IEEE Trans. Magn. 50 (2014) 1000104.
[5] E.J. Skoug, M.S. Meyer, F.E. Pinkerton, M.M. Tessema, D. Haddad, J.F. Herbst, J. Alloy. Compd. 574 (2013) 552.
[6] E. Niu, Z.A. Chen, G.A. Chen, Y.G. Zhao, J. Zhang, X.L. Rao, B.P. Hu, Z.X. Wang, J. Appl. Phys. 115 (2014) 113912.
[7] M.Y. Xing, J.Z. Han, Z. Lin, F.W. Wan, C. Lin, S.Q. Liu, C.S. Wang, J.B. Yang, Y.C. Yang, J. Magn. Magn. Mater. 331 (2012) 140.
[8] M. Zhang, Z.B. Li, B.G. Shen, F.X. Hu, J.R. Sun, J. Alloy. Compd. 651 (2015) 144.
[9] A.K. Pathak, K.A. Gschneidner Jr., M. Khan, R.W. McCallum, V.K. Pecharsky, J. Alloy. Compd. 668 (2016) 80.
[10] W. Li, A. Li, H. Feng, S. Huang, J. Wang, M. Zhu, IEEE Trans. Magn. 51 (2015) 2103603.
[11] M.G. Zhu, R. Han, W. Li, S.L. Huang, D.W. Zheng, L.W. Song, X.N. Shi, IEEE

Trans. Magn. 51 (2015) 2104604.
[12] X.F. Zhang, J.T. Lan, Z.B. Li, Y.L. Liu, L.L. Zhang, Y.F. Li, Q. Zhao, Chin. Phys. B 25 (2016) 057502.
[13] A. Alam, M. Khan, R.W. Mccallum, D.D. Johnson, Appl. Phys. Lett. 102 (2013) 042402.
[14] S.X. Zhou, Y.G. Wang, R. Høier, J. Appl. Phys. 75 (1994) 6268.
[15] M. Ito, M. Yano, N. Sakuma, H. Kishimoto, A. Manabe, T. Shoji, A. Kato, N.M. Dempsey, D. Givord, G.T. Zimanyi, AIP Adv. 6 (2016) 056029.
[16] Z. Li, W. Liu, S. Zha, Y. Li, Y. Wang, D. Zhang, M. Yue, J. Zhang, X. Huang, J. Magn. Magn. Mater. 393 (2015) 551.
[17] A.K. Pathak, M. Khan, K.A. Gschneidner Jr., R.W. McCallum, L. Zhou, K. Sun, M.J. Kramer, V.K. Pecharsky, Acta Mater. 103 (2016) 211.
[18] J. Jin, Y. Zhang, G. Bai, Z. Qian, C. Wu, T. Ma, B. Shen, M. Yan, Sci. Rep. 6 (2016) 30194.
[19] H.W. Chang, C.H. Chen, C.C. Hsieh, W.C. Chang, J. Nanosci, Nanotechnology 11 (2011) 2756.
[20] C.J. Yan, S. Guo, R.J. Chen, D. Lee, A.R. Yan, IEEE Trans. Magn. 50 (2014) 2102605.
[21] L.H. Chu, Y. Liu, J. Li, Y.L. Ma, C.Y. Li, IEEE Trans. Magn. 48 (2012) 2092.
[22] J.F. Herbst, Rev. Mod. Phys. 63 (1991) 819.
[23] J.F. Herbst, M.S. Meyer, F.E. Pinkerton, J. Appl. Phys. 111 (2012) 07A718.
[24] G.C. Hadjipanayis, Y.F. Tao, K. Gudimetta, Appl. Phys. Lett. 47 (1985) 757.
[25] C.J. Yan, S. Guo, R.J. Chen, D. Lee, A.R. Yan, Chin. Phys. B 23 (2014) 107501.
[26] Z.B. Li, M. Zhang, B.G. Shen, F.X. Hu, J.R. Sun, Mater. Lett. 172 (2016) 102.
[28] C. Yan, S. Guo, R. Chen, D. Lee, A. Yan, IEEE Trans. Magn. 50 (2014) 2104604.
[27] Z.B. Li, B.G. Shen, M. Zhang, F.X. Hu, J.R. Sun, J. Alloy. Compd. 628 (2015) 325.
[29] J. Yamasaki, H. Soeda, M. Yanagida, K. Mohri, N. Teshima, O. Kohmoto, T. Yoneyama, N. Yamaguchi, IEEE Trans. Magn. 22 (1986) 763.
[30] K.Y. Ko, S. Yoon, J.G. Booth, J. Magn. Magn. Mater. 176 (1997) 313.
[31] J.M.D. Coey, Scr. Mater. 67 (2012) 524.
[32] Q.Y. Zhou, Z. Liu, S. Guo, A.R. Yan, D. Lee, IEEE Trans. Magn. 51 (2015) 2104304.
[33] K. Pei, X. Zhang, M. Lin, A. Yan, J. Magn. Magn. Mater. 398 (2016) 96.
[34] Z.B. Li, M. Zhang, B.G. Shen, J.R. Sun, Appl. Phys. Lett. 102 (2013) 102405.
[35] K.Y. Ko, S. Yoon, J.G. Booth, H.J. Al-kanani, S.K. Cho, J. Mater. Sci. 37 (2002) 1421.
[36] Z.B. Li, B.G. Shen, M. Zhang, Y. Zhang, F.X. Hu, J.R. Sun, Appl. Phys. Lett. 106 (2015) 042403.
[37] A. Waske, B. Schwarz, N. Mattern, J. Eckert, J. Magn. Magn. Mater. 329 (2013) 101.
[38] H. Kronmüller, K.D. Durst, M. Sagawa, J. Magn. Magn. Mater. 74 (1988) 291.